

# Optimizing Frequent Checkpointing via Low-Cost Differential for Distributed Training Systems

Chenxuan Yao, Yuchong Hu, Feifan Liu, Zhengyu Liu, Dan Feng

**Abstract**—Distributed training of large deep-learning models often leads to failures, so checkpointing is commonly employed for recovery. State-of-the-art studies focus on frequent checkpointing for fast recovery from failures. However, it generates numerous checkpoints, incurring substantial costs and thus degrading training performance. Recently, differential checkpointing has been proposed to reduce costs, but it is limited to recommendation systems, so its application to general distributed training systems remains unexplored.

We propose LowDiff, an efficient frequent checkpointing framework that *reuses* compressed gradients, serving as differential checkpoints to reduce cost. Furthermore, LowDiff incorporates a batched gradient write optimization to persist these differentials to storage efficiently. It also dynamically tunes both the checkpoint frequency and the batching size to maximize performance. In non-compression scenario, We further propose LowDiff+ with a layer-wise gradient reusing and snapshotting approach and a CPU-based asynchronous persistence strategy, enabling frequent checkpointing without gradient compression. Experiments on various workloads show that LowDiff can achieve checkpointing frequency up to per iteration with less than 3.1% runtime overhead.

## I. INTRODUCTION

Deep learning has demonstrated remarkable capabilities in the fields of computer vision [20], [49], natural language processing [6], [14] and so on. Recently, the advent of large models like ChatGPT [37] and GPT-4 [38] has captivated both academic and industrial attention. To efficiently train the large models, *distributed training systems* [26], [27], [44], [46] are widely deployed across workers (or nodes) to accelerate the training process, which iterates over a dataset many times (i.e., *epochs*), each containing multiple *iterations*. Nevertheless, distributed training often requires many nodes and a long training time, leading to frequent failures [55]. For instance, a Microsoft study reveals that the mean time between failures (MTBF) in multi-tenant GPU clusters can range from minutes to days [23]; similarly, OPT-175B, equipped with 992 NVIDIA A100 GPUs, experienced 112 failures during its 90-day training period—averaging nearly two failures per day [34].

To handle failures, *checkpointing*, which regularly writes the model state to storage (e.g., disks) for failure recovery, can confine the potential loss of the training progress to the interval between consecutive checkpoints, only requiring the recovery of the remaining progress. Traditional checkpointing saves the model states (including the model parameters and optimizer parameters) at epoch boundaries, but an epoch often runs for hours, so the epoch-level checkpointing often results in hours of GPU computation wasted on average for every failure recovery [36].

Consequently, state-of-the-art checkpointing studies on fast recovery (e.g., Checkfreq [36] and Gemini [54]) aim to increase the frequency of checkpointing from epochs to iterations (we call *frequent checkpointing*). Nevertheless, the frequent checkpointing generates a considerable number of checkpoints, whose creation and transmission will incur substantial computational and communication costs, and thus hinder the training process significantly. Recent studies on reducing such costs (e.g., Check-N-Run [15]) introduce *differential checkpointing* (DC for short), which only tracks and checkpoints the modified part of the model to reduce the checkpoint size, into recommendation systems by leveraging its unique sparse features.

However, when deploying DC with high frequency in general distributed training systems, we observe two challenges arising: (1) without the help of sparse features, frequent DC incurs significant computation cost required for compressing the original differentials into smaller ones (i.e., *compressed differentials*), thus hindering the training process, and (2) frequent DC causes significant training stalls, as frequent checkpoint writes incur substantial transmissions which can not be overlapped with training, thus degrading the training performance (see §III-A for details).

Fortunately, we also have two findings from the gradient compression techniques [7], [9], [18], [35], [50] widely used in distributed training systems for communication efficiency: (1) the compressed gradients can be reused to construct the compressed differentials for general deep-learning models. (2) Using compressed gradients eliminates the data dependency between training and checkpointing, enabling them to run in parallel. Moreover, the size of compressed gradients is significantly smaller than that of compressed differentials (see §III-B for details).

Therefore, to address the above challenges, the corresponding findings inspire us to leverage the compressed gradients in distributed training systems for low-cost differential checkpointing, so as to improve the overall training performance. Our motivation is that the compressed gradients can act as the compressed differentials with no DC computation cost and with a lower DC transmission cost. Based on the findings, we propose LowDiff, an efficient frequent checkpointing framework, whose main idea is to *reuse* the compressed gradients to serve as differential checkpoints, which not only eliminates the computation cost for differential compression (via reusing) but also reduces the transmission cost for DC writes (due to smaller-size gradients than differentials). Further, to enhance LowDiff, we accelerate the checkpoint writes via gradient batching and optimize the checkpointing performance by tun-

ing the checkpoint frequency and batching size.

In scenarios without gradient compression, we further investigate how to efficiently reuse gradients for frequent DC construction and propose LowDiff+. In this case, directly compressing differentials would incur high computation costs, so we reuse and snapshot gradients as they are generated layer by layer during the backward pass, overlapping their offloading with computation, thus enabling a fine-grained reusing and snapshotting approach. Meanwhile, the model state is reconstructed in CPU memory by the reused gradients and regularly persisted to storage, both in parallel with ongoing GPU training, thus enabling high-frequency in-memory checkpointing and asynchronous persistence.

Our contributions include:

- We observe two challenges in computation and transmission when deploying differential checkpointing directly in general distributed training systems with high frequency. Motivated by the two corresponding findings of compressed gradients, we propose LowDiff, which reuses compressed gradients to act as the compressed differential checkpoints, thereby lowering the cost (§III).
- We perform an analysis of LowDiff, showing that gradient reuse eliminates the data dependency and enables parallel execution between checkpointing and training. Through measurement, we further demonstrate that checkpointing can be overlapped with the training iteration, allowing checkpointing to execute concurrently with training (§IV).
- We design LowDiff, which realizes the reuse of compressed gradients via a queue structure and facilitates zero-copy transmission between the training and checkpointing processes. Atop LowDiff, we propose a batched gradient writing optimization by merging compressed gradients in CPU memory before persisting to storage. We also design a checkpointing configuration optimization to minimize the wasted GPU time (§V).
- We further propose LowDiff+ for efficient gradient reuse without compression. By exploiting the layer-by-layer generation of gradients during training, we design a layer-wise gradient reusing and snapshotting approach. We also reconstruct a model state in CPU memory, performing high-frequency in-memory checkpointing and asynchronous persistence (§VI).
- We implement LowDiff and LowDiff+ atop DeepSpeed, open-sourced at <https://github.com/YuchongHu/LowDiff>. Experiments on various models show that LowDiff and LowDiff+ can achieve checkpointing as frequently as once per iteration with less than minimal runtime overhead. Compared to the state-of-the-art methods, LowDiff and LowDiff+ can shorten training time by up to 89.2% and 81.7% under high checkpointing frequencies (§VII & §VIII).

## II. BACKGROUND AND RELATED WORK

### A. Basics of Distributed Training Systems

A deep neural network (DNN) contains many model *parameters*. Training DNN models is the process of determining the optimal set of weights and biases that minimizes the loss function of the model, which measures the difference

between the model predictions and the target values. The training process starts with a set of parameters and proceeds iteratively over a dataset many times (i.e., *epochs*), each of which contains multiple *iterations*, with an *optimizer* being used to adjust the parameters based on the *gradients* (i.e., derivatives of the loss function w.r.t. model parameters)

To accelerate the training process of large models and datasets [28], [44], [46], [56], *distributed training systems* are commonly adopted to distribute computations and data across multiple GPUs. Specifically, distributed training has four steps for the  $t$ -th iteration:

- *Forward pass*. The model parameters  $x_t$  is applied to the input data set  $X$  to obtain the prediction  $Y$  as:

$$Y = Forward(x_t, X). \quad (1)$$

- *Backward pass*. A loss function is used to calculate the gradient  $G_{i,t}$  on  $i$ -th worker, satisfying that

$$G_{i,t} = Backward(x_t, Y). \quad (2)$$

Then the gradients of workers are synchronized through communication primitives, satisfying that

$$G_t = Sync(G_{i,t}). \quad (3)$$

- *Model update*. The optimizer (e.g., Adam [24]) uses the synchronized gradient  $G_t$  to update the *model state* (denoted by  $M_t$ ), which contains the model parameters  $x_t$  and the optimizer parameters  $o_t$  (i.e.,  $M_t = (x_t, o_t)$ ), satisfying that

$$M_{t+1} \leftarrow M_t + Adam(G_t). \quad (4)$$

Here, we specially introduce the widely used optimizer, Adam. The Adam optimizer maintains the first-order and second-order moments (i.e., the mean and variance of the gradients), and each has the same size as the model parameters, denoted by  $\Psi$ . Therefore, Adam requires an additional  $2\Psi$  parameter storage beyond the model itself, which will support one of our findings in §III-B.

### B. Checkpointing Techniques

When training large models, failures frequently occur in distributed training systems due to extensive computational resources and long training times. To handle frequent training failures, *checkpointing*, a widely used technique in common training frameworks (e.g., PyTorch [39] and Tensorflow [1]), has been extensively studied [8], [15], [19], [32], [36], [53], [54]. It regularly copies the model state to local storage or remote storage during training. During recovery from the failure, all GPUs load the latest checkpoint and rerun the remaining process until the point of failure. To evaluate checkpointing performance, recent studies (e.g., [19]) define the *wasted time* metric as the sum of the recovery time from the latest checkpoint and the steady-state overhead (i.e., the GPU time for checkpointing when no failures have happened). **Frequent checkpointing.** Traditional checkpointing is performed at the granularity of epochs, but an epoch may run for hours, thus incurring substantial wasted time for every failure [36]. Thus, state-of-the-art studies [36], [54] that aim for fast recovery increase the checkpointing frequency from epochs to

iterations, which we call *frequent checkpointing* in this paper. The state-of-the-art systems are specified as follows:

Checkfreq [36] decouples checkpointing into *snapshot* and *persist* operations, and pipelines them with computation to enable frequent checkpointing. Specifically, the snapshot operation copies model parameters from GPU to CPU memory, while the persist operation asynchronously writes the snapshot to persistent storage. This design allows Checkfreq to create a checkpoint every 14–19 iterations.

Gemini [54] improves frequent checkpointing with the help of the CPU memory of the host machine and proposes a checkpointing traffic scheduling algorithm to mitigate the impact on model training. In this way, Gemini increases the checkpoint frequency over Checkfreq by up to  $8\times$ , even per-iteration frequency.

PCcheck [52] enables checkpointing as frequently as every 10 iterations by checkpointing to persistent main memory (PMEM). PCcheck utilizes concurrent checkpoints and minimizes time per checkpoint using pipelining techniques and multiple threads.

Just-in-time checkpointing [19] diverges from prior frequent checkpointing techniques. Instead of saving model states at regular intervals, Just-in-time checkpointing initiates a checkpoint only when a failure is detected and assumes redundancy across workers to ensure fault tolerance.

Despite the fast recovery of frequent checkpointing, the frequent creation and transmission of checkpoints will incur substantial costs, thus degrading the training performance. In this paper, our main goal is to lower the costs of frequent checkpointing for high-performance training.

**Differential checkpointing.** A recent study, Check-N-Run [15], on reducing the checkpointing costs introduces *differential checkpointing* (DC for short), which records the part of the model that is modified only during the last checkpoint interval so as to reduce the checkpoint size.

Specifically, DC saves its model state as *full checkpoint* ( $C^F$ ) regularly. DC also saves its *differential checkpoint* of the  $t$ -th iteration (denoted by  $C_t^D$ ) at an iteration-level high frequency as

$$C_t^D = M_{t+1} - M_t. \quad (5)$$

Then the model state  $M_t$  at the  $t$ -th iteration can be reconstructed by merging the full and all differential checkpoints as

$$M_t = C^F + C_1^D + C_2^D + \dots + C_{t-1}^D. \quad (6)$$

However, we note that Check-N-Run implements DC only in recommendation systems, since the recommendation model has a unique property that its embedding table has a high sparsity such that DC is particularly well suited for recommendation models where only a *small part* of the model parameters are updated after each iteration.

In contrast, general DNN models have to be updated *entirely* after each iteration since gradients are computed for all the model parameters, so in this case, deploying DC has to highly compress the differentials, leading to substantial computational cost, while higher frequency incurs more cost (see §III-A).

In this paper, we focus on how to enable low-cost DC for general DNN models, so as to extend the DC technique

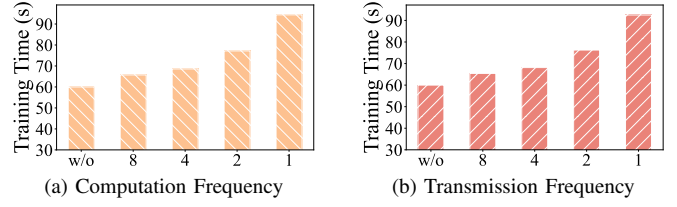


Fig. 1: Impacts of DC computation and transmission frequency (in iterations) on training performance of GPT2-L.

from recommendation systems to general distributed training systems.

### C. Gradient Compression Techniques

*Gradient compression* techniques have been widely used in high-performance distributed training systems [3], [4], [9], [13], [16], [17], [30], [31], [47], [48], [50], [51] to significantly reduce the communication overhead of the gradient synchronization in backward pass (see §II-A and Equation (3)). Two representative compression approaches are *Sparsification* [3], [51], which selects only a subset of the elements of the gradient, and *Quantization* [5], [13], which reduces the number of bits of each element of the gradient.

In this paper, we will observe that the costs of deploying DC in distributed training can be largely reduced by leveraging gradient compression, which motivates our main idea (see §III-C for details).

## III. OBSERVATIONS AND MOTIVATION

In this section, we present two challenges of deploying frequent differential checkpointing (DC) in distributed training systems (§III-A) and discuss two corresponding findings from the gradient compression technique (§III-B). We also provide an analysis of the data dependency between training and checkpointing. Finally, we demonstrate how these observations motivate our main idea to address the challenges (§III-C).

### A. Challenges of DC in General Training

As stated in §II-B, DC may incur high costs when deployed in general distributed training systems without the help of the sparsity feature in recommendation systems, so we conduct measurements to observe that show the challenges of DC in general distributed training systems, especially under high frequency. We conduct our measurement on eight NVIDIA A100 GPUs with a 25Gbps network [54]. We evaluate a typical large-model training task GPT2-L [41], with a common differential checkpointing scheme (see Equation (6)). Detailed setups are shown in §VIII-A.

**Challenge 1: Frequent DC incurs significant computation cost for highly compressing differentials.** In the absence of the sparsity feature’s support, DC has to apply the highly compressed scheme (compression ratio  $\rho = 0.01$  [15]) to the differentials (called *compressed differentials*), thus degrading the training performance. To measure the impact of compression computation cost on training, Figure 1(a) shows the training

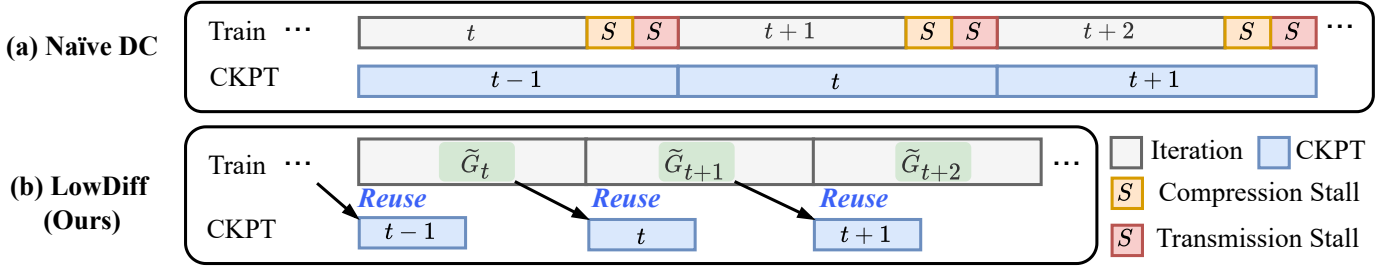


Fig. 2: Motivating example of LowDiff.

time of cases without compression and with different compression frequencies (e.g., 8 iteration compression frequency means the compression is performed every 8 iterations). We see that compared to the case without compression, the case with compression slows down the training process greatly by 13% ~ 57%, while higher frequency incurs much slower training.

**Challenge 2: Frequent DC causes significant transmission cost due to frequent checkpoint writes.** Frequent DC needs to write the differential of model state to storage frequently, which blocks the training process frequently and incurs substantial transmission overhead, since the model update has to wait for the snapshotting of checkpoint [36], [53]. To measure the impact of transmission cost on training in terms of frequency, Figure 1(b) shows the training time of cases without differential transmission and with different differential transmission frequencies. We observe that compared to the case without differential transmission, the case with differential transmission slows down the training process by 12% ~ 54%, while higher frequency incurs slower training.

### B. Findings from Gradient Compression

To address the above challenges, we resort to the gradient compression technique, which is widely studied and deployed in both academia and industry (§II-C), and obtain the following two findings.

**Finding 1: The compressed gradients can directly construct the compressed differentials for general DNN models.** Gradients of a general DNN model are used to adjust the model state via the optimizer (e.g., Adam), so based on Equation (4), we have  $Adam(G_t) = M_{t+1} - M_t$ . Meanwhile, the differential checkpoint of the  $t$ -th iteration  $C_t^D = M_{t+1} - M_t$  based on Equation (5). Thus, we have:

$$C_t^D = Adam(G_t). \quad (7)$$

Therefore, the compressed version of the differential checkpoint  $C_t^D$  can be directly constructed via the optimizer by the compressed gradient  $\tilde{G}_t$ , which can be obtained in advance by the gradient compression operation.

**Finding 2: The compressed gradients are one-third of the compressed differentials in size.** As mentioned in §II-A, if the model parameters are of size  $\Psi$ , the Adam optimizer parameters occupy  $2\Psi$ , making a full checkpoint  $3\Psi$  in total. Next, Equation (6) implies that a differential checkpoint has

the same size as the full one, i.e.,  $3\Psi$ , which includes the model parameters and the Adam optimizer parameters. By contrast, the size of a gradient is equal to that of the model parameters, i.e.,  $\Psi$ . Therefore, applying the same compression method results in a compressed gradient three times smaller than a compressed differential checkpoint.

### C. Main idea

Challenges 1 and 2 show that frequent DC has high computation and transmission cost, including *compression stalls* (caused by DC’s differential compression) and *transmission stalls* (caused by DC’s writes). Figure 2(a) illustrates that during a 3-iteration training, DC has three compression stalls and three transmission stalls, hindering the training process.

Findings 1 and 2 show that the compressed gradient can construct the compressed differentials, and its size is much smaller than the compressed differential. Thus, the compressed gradient can be leveraged to *act as* the compressed differential checkpoint of DC, so as to (1) remove the compression stalls via eliminating DC’s differential compression, and (2) reduce or even remove the transmission stalls since the small-size compressed gradient is likely to enable DC’s transmission to be overlapped with the training process.

Therefore, we propose LowDiff, a low-cost differential checkpointing framework, whose main idea is to *reuse* the compressed gradients to act as the differential checkpoints with no DC compression cost and with a lower DC transmission cost. Figure 2(b) illustrates that during a 3-iteration training, LowDiff has no compression and transmission stalls by reusing  $\tilde{G}_t$ ,  $\tilde{G}_{t+1}$  and  $\tilde{G}_{t+2}$  as three differential checkpoints, speeding up the training.

While LowDiff provides a low-cost DC way based on gradient reuse, its integration into training systems, particularly the feasibility of concurrent execution with the training process, requires further analysis. We next analyze such concurrency in §IV.

## IV. ANALYSIS

By incorporating the main idea of gradient reuse (§III), LowDiff aims to enable the DC process to run concurrently with model training, thereby minimizing potential stalls. To confirm the feasibility of such parallelism, we analyze our proposed strategy from two key aspects:

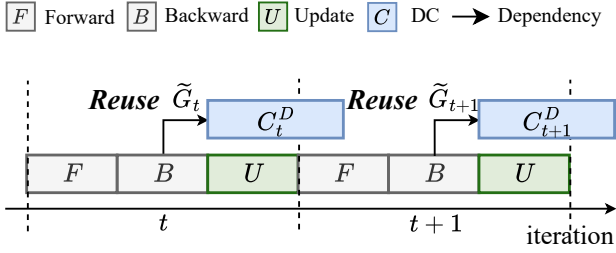


Fig. 3: LowDiff’s DC can run in parallel with forward pass(F), backward pass(B), and model update(U).

- **Parallelism property:** it ensures no data dependencies block concurrency with training iterations.
  - **Execution time overlap:** it reveals whether the checkpointing cost can be effectively hidden within the training time.
- We provide a detailed analysis of these two aspects as follows.

#### A. Parallelism Analysis

**Necessity of Parallelism Analysis.** Checkpointing can be executed with the forward and backward passes which do not modify the model state [36], but it cannot run in parallel with model update which directly writes to it [53]. In other words, checkpointing is data-dependent on the model update [53]. The reason is that it must read the model state after model updates (Read-after-Write [21], RAW dependency), and the model update at the next iteration must write the model state after checkpointing completes its read (Write-after-Read [21], WAR dependency). Consequently, the two dependency patterns incur training stalls, preventing from paralleling checkpointing with model update. Prior studies [36], [53], [54] design their checkpointing strategies based on these data dependencies to pipeline training and checkpointing.

Consequently, it is necessary to carefully analyze: (1) the data dependency introduced by our reuse strategy and (2) the parallelism property of LowDiff’s DC, specified as follows.

**(1) LowDiff’s DC can eliminate the WAR dependency.** We next analyze current DC’s WAR dependency with next iteration’s model update, backward, and forward pass.

- **Model update:** as described in §II-A, the model update (Equation (4)) only requires read-only access to the gradient. Because LowDiff checkpoints only the compressed gradient, leveraging gradient reuse, the original Write-after-Read (WAR) dependency is eliminated because the checkpointing process no longer needs to read the model state ( $M_t$ ). Instead, it just reads the compressed gradient ( $\tilde{G}_t$ ), which is available in the backward pass and will not be changed after. Since both the checkpointing and model update are read-only consumers of the gradient, they can operate in parallel without conflict.
- **Backward pass:** LowDiff’s gradient reuse strategy introduces no additional WAR dependency on backward pass, since each gradient  $G_t$  is finalized within its iteration and never modified thereafter. Specifically, once a gradient  $G_t$  is generated in the current iteration ( $t$ ), it is final and will not be modified by subsequent steps. The backward pass of the  $t+1$ -th iteration (Equation (2)) does not read or depend

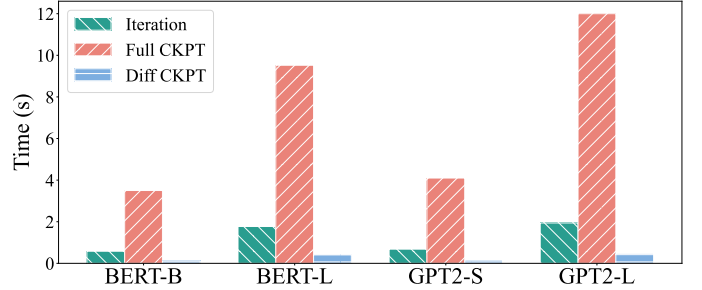


Fig. 4: Time of iteration, full checkpointing, and differential checkpointing.

on  $G_t$ ; it generates a completely new gradient ( $G_{t+1}$ ) from scratch and won’t change the  $G_t$ . Therefore, the DC’s read of  $G_t$  does not conflict with the  $B$ ’s write of  $G_{t+1}$  at  $t+1$ -th iteration, allowing LowDiff’s DC to run in parallel with the next iteration’s backward pass.

- **Forward pass:** The forward pass (Equation (1)) doesn’t involve gradient, so there is no WAR dependency between LowDiff’s DC and forward pass.

**(2) LowDiff can run in parallel with forward pass, backward pass, and model update.** To visualize the parallelism benefit from data dependency, Figure 3 shows the execution timeline with LowDiff. We see that the DC task ( $C_t^D$ ) at the  $t$ -th iteration is no longer coupled with the model update ( $U$ ) or the following iteration (no dependency arrow from DC to training). Instead, the reusing operation on compressed gradient ( $\tilde{G}_t$ ) begins immediately after the backward pass ( $B$ ), running in parallel with the model update and subsequent iteration’s forward pass(F), backward pass (B), and model update(U). This parallelism property effectively transforms LowDiff’s DC from a blocking operation to a parallel execution with training, thereby eliminating the synchronization stalls previously caused by the WAR dependency.

#### B. Overlap Analysis

**Necessity of Overlap Analysis.** Beyond its parallelism property, LowDiff can perform even better if the checkpointing process is fast enough to be hidden by the training iteration, thus minimizing DC’s cost. Specifically, the time required to checkpoint a compressed gradient (denoted as  $C$ ) should be shorter than a single training iteration (denoted as  $F+B+U$ ), similar to the Microsoft study [36].

Consequently, it is also necessary to analyze the potential of overlapping, so we first (1) take a measurement analysis of training time, full checkpointing, and DC time, as well as (2) discuss why the overlap can be practically feasible.

**(1) The checkpointing of compressed gradients can be overlapped with training.** Following the measurement setup in §III-A, we measure the iteration time, full checkpointing time and differential checkpointing time on BERT-B, BERT-L, GPT2-S, and GPT2-L. As shown in Figure 4, the DC time is only 20.5%, 22.1%, 23.1%, and 24.6% of the corresponding training iteration time for these models. This indicates that in most cases, the checkpointing process can be fully overlapped with training iterations without introducing noticeable stalls.

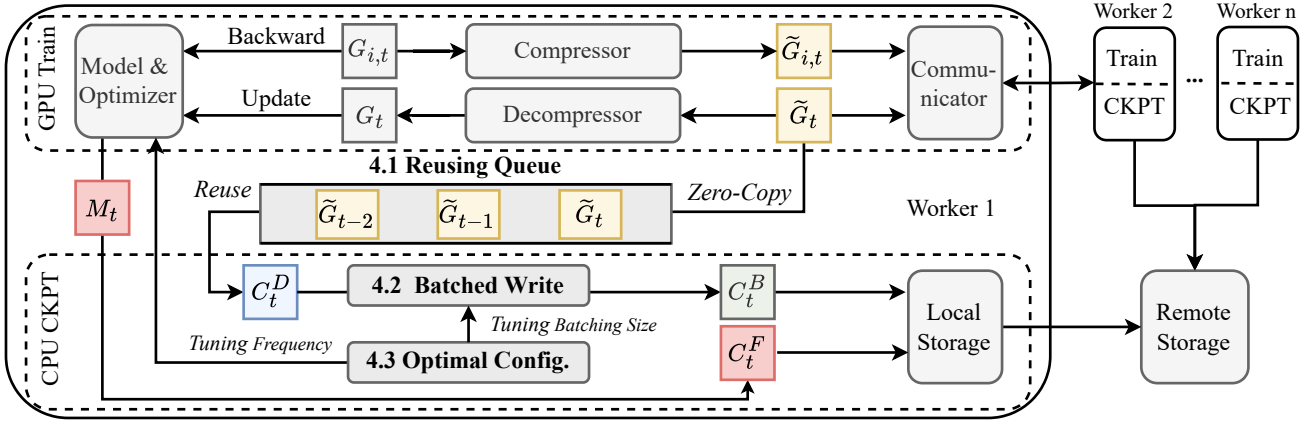


Fig. 5: Architecture of LowDiff

(2) **Modern hardware makes the overlap practically feasible.** NVMe SSDs based on PCIe 4.0 offer write speeds around 5 GB/s (and up to 12 GB/s for PCIe 5.0, with RAID 0 configurations being even faster). Given that LowDiff’s compressed-gradient checkpoints are relatively small (several hundred MBs to a few GBs, as evaluated in §VIII), the theoretical I/O write time is typically under 1 second. This duration is significantly shorter than that of a full training iteration [54].

Based on the above analysis, we confirm that the concurrent execution between LowDiff’s DC and training is theoretically feasible. While this analysis establishes the feasibility of frequent DC, the detailed design of LowDiff will be presented in §V.

## V. DESIGN

We design LowDiff based on the main idea in §III-C with the following design goals.

- **Lowering the costs of DC.** LowDiff reduces or even eliminates the computation and transmission costs of compressed differential checkpoints by reusing compressed gradients (§V-A).
- **Enhancing DC performance.** LowDiff accelerates the differential checkpointing under high frequency via batched gradient writing optimization (§V-B).
- **Minimizing the wasted time.** LowDiff minimizes the wasted time by analytically tuning the full checkpointing frequency and gradient batching size (§V-C).

Figure 5 shows the architecture of LowDiff. Each worker has two processes: Training and Checkpointing, connected via Reusing Queue for gradient reuse. Training first generates the local gradient, compresses it in Compressor, and synchronizes it across workers via Communicator. The synchronized compressed gradient  $\tilde{G}_t$  is put into Reusing Queue via zero-copy technique for reuse in checkpointing and is also decompressed by Decompressor to update the model state. Training checkpoints the model state  $M_t$  regularly as full checkpoints  $C_t^F$ . Checkpointing snapshots compressed gradients from Reusing Queue to form differential checkpoints  $C_t^D$ , which Batched Writing module caches in CPU memory and aggregates into a single batched

differential checkpoint  $C_t^B$ . Both the full checkpoint frequency and batching size are dynamically tuned by Optimal Configuration module. Finally, the batched differential and full checkpoints are persisted to local or remote storage.

### A. Reusing Compressed Gradients

**Design requirements.** The reuse of the compressed gradients to act as the compressed differentials imposes two main system-level requirements: *Requirement 1: Ensuring sequential order for reusing gradients.* Since the compressed gradients are generated sequentially during training and differential checkpoints also need to capture model state changes sequentially (see Equation (6)), it is necessary to preserve the sequence of the compressed gradients to ensure that they act as the differentials in the correct sequential order. *Requirement 2: Facilitating transmission between training and checkpointing.* To avoid performance degradation, the reused gradients need to be transmitted between training and checkpointing with low communication overhead.

**Reusing queue structure.** To meet *Requirement 1*, we design a queue-based data structure, referred to as the compressed gradient *Reusing Queue* in Figure 5. Specifically, the first-in-first-out (FIFO) property of the queue naturally aligns with the iterative nature of training and checkpointing, ensuring that gradients are reused in the correct order. In addition, the implementation of the queue structure in PyTorch also helps meet *Requirement 2*, which will be specified below.

**Reusing with zero-copy optimization.** To meet *Requirement 2*, we use the CUDA Inter-Process Communication (IPC) queue in PyTorch to implement a zero-copy mechanism. This allows GPU memory to be shared between training and checkpointing without extra copying, significantly reducing communication overhead. Specifically, the queue serves as a high-level data structure for reusing compressed gradients, but only transmits the memory handle. It relies on the CUDA IPC library to share the gradient’s GPU memory handle across processes, avoiding additional I/O overhead from memory copying. In PyTorch, this can be achieved with `torch.multiprocessing.Queue()`, where the inter-process communication creates an IPC handle when a tensor is enqueued and reopens it when dequeued.

---

**Algorithm 1** Reusing in LowDiff
 

---

**Require:** Model state  $M_t$  at iteration  $t$ , Gradient  $G_{i,t}$  at worker  $i$ , Reusing queue  $Q$ , Full checkpoint  $C_t^F$ , Differential checkpoint  $C_n^D$  at iteration  $n$ , Compressor  $Comp$ , Decompressor  $Comp^{-1}$ .

```

1: function TRAINING PROCESS
2:   for all  $t$  do
3:      $G_{i,t} \leftarrow \text{Backward}(x_t)$ 
4:      $\tilde{G}_{i,t} \leftarrow \text{Comp}(G_{i,t})$  ▷ Compress
5:      $\tilde{G}_t \leftarrow \text{Sync}(\tilde{G}_{i,t})$  ▷ Synchronize
6:      $\mathbf{Q.put}(\tilde{G}_t)$  ▷ Zero-Copy
7:      $G_t \leftarrow \text{Comp}^{-1}(\tilde{G}_t)$  ▷ Decompress
8:      $M_{t+1} \leftarrow M_t + \text{Adam}(o_t, G_t)$  ▷ Update
9: function CHECKPOINTING PROCESS
10:  while  $\tilde{G}_t \leftarrow \mathbf{Q.get}$  do ▷ Reusing
11:     $C_t^D \leftarrow \text{Save}(\tilde{G}_t)$  ▷ Diff CKPT
12:     $C_t^F \leftarrow \text{Save}(M_t)$  ▷ Full CKPT Regularly
13: function RECOVERY PROCESS
14:   $M_t \leftarrow \text{Load}(C_t^F)$  ▷ Load Full CKPT
15:  for  $j \leftarrow t, \dots, n$  do ▷ Restore to Latest
16:     $\tilde{G}_j \leftarrow \text{Load}(C_j^D)$  ▷ Load Diff CKPT
17:     $G_j \leftarrow \text{Comp}^{-1}(\tilde{G}_j)$  ▷ Decompress
18:     $M_{j+1} \leftarrow M_j + \text{Adam}(G_j)$  ▷ Diff Merge
19:  return  $M_n$ 

```

---

**Design details** Algorithm 1 specifies the following details of reusing compressed gradients, including training, checkpointing, and recovery processes.

**Training process.** After performing a backward pass and generating the gradient  $G_{i,t}$  of worker  $i$  at the  $t$ -th iteration (Lines 1-3), the training process compresses  $G_{i,t}$  into  $\tilde{G}_{i,t}$  for communication (Line 4). Then, the compressed gradient is synchronized across all workers using a collective communication primitive (e.g., Allgather or Allreduce) (Line 5). Following synchronization, the training process puts the compressed gradient  $\tilde{G}_t$  into Reusing Queue  $Q$  (Line 6), which will be transmitted to the checkpointing process with *zero-copy*. Finally, the training process decompresses the gradient (Line 6), updates the model state based on the gradient (Line 8), and proceeds to the next iteration.

**Checkpointing process.** The checkpointing process repeatedly retrieves the compressed gradients from Reusing Queue  $Q$  to CPU memory (Line 11). Subsequently, the checkpointing process determines whether to merge the compressed gradient into batched differential checkpoints (detailed in §V-B). After that, it invokes `torch.save` to persist the compressed differential checkpoints  $C_t^D$  (Lines 12-14) to storage. The model state is also regularly checkpointed as a full checkpoint  $C_t^F$  at the  $t$ -iteration (Line 15).

**Recovery process.** During recovery, the recovery process first loads the latest full checkpoint  $C_t^F$  at the  $t$ -th iteration to restore the model state  $M_t$  (Line 17). Then, the compressed gradient  $\tilde{G}_j$  is retrieved from the differential checkpoint  $C_j^D$  at the  $j$ -th iteration (Line 20) and decompressed into gradient  $G_j$  (Line 21). Subsequently, the model state is restored from  $M_j$  to  $M_{j+1}$  at the  $(j)$ -th iteration by the optimizer and gradient

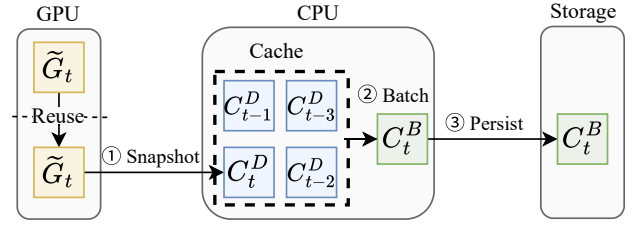


Fig. 6: Batched gradient write optimization

(Line 21). By repeating this process for  $n$  iterations (Lines 18-23), where compressed gradients from differential checkpoints are successively loaded and applied, the model state is finally restored to  $M_n$  (Line 24), thus recovering the training from failures.

### B. Batched Gradient Writing Optimization

**Limitations of LowDiff.** We find that LowDiff in §V-A still has two limitations:

- Limitation 1: Many writes due to frequent DC. The high frequency leads to numerous differential checkpoints, which incur significant write overhead.
- Limitation 2: As analyzed in §IV-A, avoiding the WAR dependency requires temporarily retaining the compressed gradient  $\tilde{G}_t$  for the DC operation. Consequently, frequent DCs cause this gradient buffer to remain occupied while waiting for the write to storage, leading to extra GPU memory consumption.

we provide the batched write and offloading strategy to address the corresponding limitation as follows.

**Batched write.** To address Limitation 1, we can batch multiple writes of compressed gradients (reused as differential checkpoints) into a single write operation, with the help of the widely-used gradient accumulation technique [2], [22], [30] where the gradients of the same shape and size can be accumulated. Note that the above batching scheme, which benefits DC writes, cannot work for traditional checkpointing that only saves full checkpoints, since if a new full checkpoint comes, the previous full checkpoints become obsolete and can be discarded without the need to accumulate them.

**Offloading batching to CPU.** To address Limitation 2, we adopt a classic GPU-CPU offloading scheme [42] that offloads the batching operation to the CPU and caches the compressed gradients in CPU memory, thus reducing the GPU memory cost caused by frequent checkpointing. Note that the batching operation can be easily handled by the CPU since the operation mainly involves the addition of compressed gradients.

**Design details.** To solve *Limitation 1* & *2*, we design a batched gradient writing optimization, which offloads multiple compressed gradients from GPU to CPU memory, and then aggregates them into batched writes to storage. As shown in Figure 6, we specify the batched gradient writing optimization of LowDiff in three steps:

**Step ①: Offloading gradients to CPU memory.** After the training process transmits compressed gradients  $\tilde{G}_t$ , the checkpointing process retrieves the GPU memory handles and offloads the gradients to CPU memory. After offloading, the

FCF \ BS	1	2	3	4	5	6
10	1.258	<b>1.226</b>	1.279	1.330	1.408	1.513
20	1.052	<b>1.000</b>	1.031	1.085	1.149	1.202
50	1.394	1.290	<b>1.255</b>	1.312	1.387	1.481
100	1.916	1.783	<b>1.712</b>	1.752	1.869	1.952

TABLE I: Normalized wasted time with different full checkpoint frequency (FCF) and batching size (BS).

checkpointing process closes the handle of  $\tilde{G}_t$  and frees the corresponding GPU memory.

**Step ②: Batching gradients in buffer.** The compressed gradients, which are reused to act as differential checkpoints  $C_t^D$ , are buffered in CPU memory, awaiting batching. Once the batching size is reached (e.g., the size is four in Fig 6), the checkpointing process groups the buffered differential checkpoints  $C_t^D$ ,  $C_{t-1}^D$ ,  $C_{t-2}^D$ , and  $C_{t-3}^D$  into a batch checkpoint  $C_t^B$ .

**Step ③: Writing batched checkpoint to storage.** The checkpointing process extracts the batched differential checkpoint  $C_t^B$  from the CPU buffer and writes it to storage in a single I/O operation.

### C. Optimizing Checkpointing Configuration

**Insight into configuring LowDiff.** Note that recent studies on optimizing the checkpointing performance only focus on configuring the checkpointing frequency (e.g., [19]). However, we observe an insight that LowDiff’s checkpointing performance will also rely on the *batching size*, i.e., the amount of the batched gradients every batching, introduced in §V-B. To verify the insight, we take another measurement analysis with the same setting as that in §III-A. Table I shows the results of the wasted time, which evaluates the checkpointing performance (see §II-B), under different batching sizes and checkpointing frequencies for full checkpoint (called *full checkpoint frequency*, FCF for short). Note that all the results are normalized by comparing them to the lowest wasted time.

We first see that when FCF is too low ( $FCF = 10$ ) or too high ( $FCF = 100$ ), the wasted time will be increased, since a low FCF will incur high recovery time while a high FCF will incur high steady state overhead (GPU time). Thus, we need to tune FCF to minimize the wasted time, which has been found by Microsoft [19].

More importantly, under the same FCF (i.e., in the same row), we also need to tune the batching size (BS for short) for minimizing the wasted time. For example, when  $FCF = 10$  or 20, the wasted time is minimal when  $BS = 2$ ; when  $FCF = 50$  or 100, the wasted time is minimal when  $BS = 3$ . The reason is that a low BS still incurs many writes due to insufficient batching, while a high BS makes one failure cause many gradients within the batch to be lost.

Therefore, we need to tune both FCF and BS to minimize LowDiff’s wasted time. For example, the wasted time in Table I achieves its minimum when  $FCF = 20$  and  $BS = 2$ .

**Configuration Modeling.** To find the configuration of FCF and BS for minimizing the wasted time, we model the configuration by constructing the expression of the wasted

time with respect to both FCF ( $f$ ) and BS ( $b$ ) variables. We also list the constant parameters of distributed training with differential checkpointing: the number of GPUs  $N$ , the mean time between failures  $M$ , the checkpointing write bandwidth  $W$ , a full checkpoint size  $S$ , the total run-time for a training job  $T$ , the time to load a full checkpoint  $R_F$ , and the time to merge a differential checkpoint  $R_D$  with the full one.

The following expression can be obtained based on the two variables and the constant system parameters above:

- The number of failures for a training job =  $\frac{T}{M}$ .
- The time of writing a full checkpoint =  $\frac{S}{W}$ .
- The number of full checkpoints during training =  $f \times T$ .
- The wasted work which is re-processed upon the last checkpoint across all GPUs =  $N \times \frac{T}{M} \times \frac{b}{2}$ . Note that half-batched checkpoints might be lost on average in the event of failures.
- The number of merging operations on average =  $\frac{1}{2}(\frac{1}{f} \times \frac{1}{b} - 1)$ . Note that the number of batched DC equals dividing the full checkpoint interval by the batching size.
- The recovery time for all nodes to load checkpoints =  $N \times \frac{T}{M} \times (R_F + R_D \times \frac{1}{2}(\frac{1}{f} \times \frac{1}{b} - 1))$ , including loading a full checkpoint and merging differential checkpoints.
- Total recovery overhead due to failures across all GPUs =  $N \times \frac{T}{M} \times ((R_F + R_D \times \frac{1}{2}(\frac{1}{f} \times \frac{1}{b} - 1)) + \frac{b}{2})$ , including loading checkpoints and re-processing the wasted work.
- Total steady state overhead for checkpointing across all GPUs =  $N \times \frac{S}{W} \times f \times T$ .

The wasted time  $T_{wasted}$  can be calculated by adding recovery overhead and steady state overhead (see §II-B):

$$T_{wasted} = \frac{NT}{M} \left( \frac{b}{2} + (R_F + \frac{R_D}{2} (\frac{1}{f \times b} - 1)) \right) + \frac{NT \times S \times f}{W}. \quad (8)$$

To minimize  $T_{wasted}$  on two variables  $f$  and  $b$ , we take the first-order partial derivatives of  $T_{wasted}$  with respect to  $f$  and  $b$ .

$$\begin{cases} \frac{\partial T_{wasted}}{\partial f} = \frac{NST}{W} - \frac{NT \times R_D}{2f^2 \times M \times b} = 0. \\ \frac{\partial T_{wasted}}{\partial b} = \frac{1}{2} - \frac{R_D}{2b^2 \times f} = 0. \end{cases} \quad (9)$$

Equation (4) can be reduced to obtain the optimal values of the full checkpointing frequency ( $f^*$ ) and batching size ( $b^*$ ) as follows.

$$(f^*, b^*) = \left( \sqrt[3]{\frac{R_D W^2}{4 S^2 M^2}}, \sqrt[3]{\frac{2 S R_D M}{W}} \right) \quad (10)$$

We will use  $(f^*, b^*)$  as the optimal configuration in LowDiff.

## VI. ENHANCEMENT

The current design of LowDiff relies on gradient compression to enable efficient gradient reuse. However, in some high-precision training scenarios, any potential accuracy degradation caused by compression is unacceptable. If the distributed training system does not inherently employ a gradient compression strategy, making it impossible to leverage compression-induced bandwidth advantages. So we also need to design a non-compression high-frequency DC strategy for above scenarios. We next present two key insights on snapshotting and persistence, followed by a detailed description of

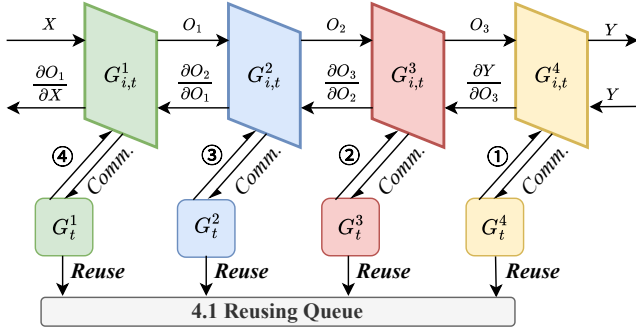


Fig. 7: Layer-wise gradient reuse.

how **LOWDiff** can be enhanced in scenarios without gradient compression (**LOWDiff+** for short).

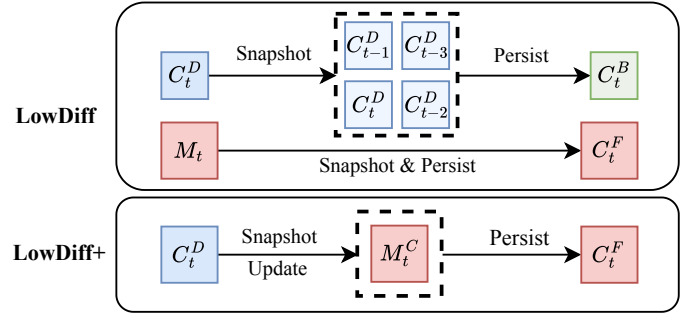
#### A. Layer-Wise Gradient Reusing and Snapshotting Strategy.

**Issue of snapshotting.** A key issue in the non-compression setting arises during the snapshot stage: unlike compressed gradients, transferring raw gradients without compression from GPU to CPU introduces heavier data movement and increases the likelihood of a stall. The snapshotting competes more directly with training for GPU and I/O resources, making overlap optimization even more critical to mitigate the training stall. To accelerate such large-scale snapshotting, we aim to design a fine-grained strategy that better overlaps gradient transmission with training.

**Insight 1: gradient can be reused layer-by-layer.** We recall that gradients are produced incrementally in the backward pass, following the reverse layer order during training, as shown in Figure 7. Instead of waiting until the entire backward pass finishes to synchronize all gradients, which would incur high latency and risk blocking training, modern frameworks (e.g., DeepSpeed [10], PyTorch DDP [28], and Horovod [46]) already exploit layer-wise gradient availability by initiating communication as soon as each layer’s gradients are produced. Inspired by this execution model, we design a fine-grained reuse strategy: once a layer’s gradient has been synchronized, we immediately reuse it to the reusing queue, snapshot it to host memory, and stream it into a differential checkpoint assembler. This granular approach enables parallel data movement, allowing concurrent snapshot writes to CPU DRAM to better utilize memory bandwidth, thereby mitigating the high transfer volume. By pipelining backpropagation, communication, gradient reuse, and snapshotting at the layer granularity, we can effectively hide checkpointing overhead behind ongoing training, thereby maximizing overlap with training and reducing stalls.

#### B. CPU-Based Asynchronous Persistence Strategy.

**Issue of persistence.** While the layer-wise strategy addresses the snapshotting issue in the non-compression setting, another issue remains: persistence of both full and differential checkpoints. The batching strategy described in §V-B accumulates small compressed updates on the CPU side before writing them out. It also periodically persists the full model state,

Fig. 8: Batching strategies of **LOWDiff** and **LOWDiff+**.

which works effectively when update sizes are small and sparse. In the non-compression setting, differential checkpoints are significantly larger, and naively batching them demands a sustained write throughput that exceeds the available storage bandwidth, making it essential to design a more efficient checkpoint merging strategy that better lowers the writing data volume.

**Insight 2: differential and full checkpoints can be batched together in CPU memory.** We find that in the non-compression setting, the differential checkpoints (i.e. gradients) and full checkpoints do not need to be persisted separately. Instead, they can be directly fused with the full model state inside CPU memory, enabling the CPU to maintain an always-up-to-date replica of the GPU model. Once gradients are merged into the CPU-resident model state, persistence only needs to occur from the CPU model to storage. By fusing gradients into the CPU-resident model state instead of persisting them separately, redundant writes of differential checkpoints are avoided, which directly reduces the overall storage volume. The different batching strategies of **LOWDiff** and **LOWDiff+** are shown in Figure 8. This strategy decouples persistence from GPU training, enabling fully asynchronous checkpointing with minimal interference to ongoing training.

#### C. Design of **LOWDiff+**

**Design details.** Based on *Insight 1 and 2*, we design **LOWDiff+** under non-compression scenarios. The architecture of **LOWDiff+** is shown in Figure 9, and its detailed algorithm is presented in Algorithm 2. In the training process, the model first performs backpropagation to calculate gradients  $G^n_{i,t}$  layer-by-layer as shown in Figure 7 (Line 5). The layer-wise gradient communication is then handled by a communication thread pool  $P_g$ , where the gradient synchronization is assigned to multiple communication threads (Line 15). Once the communication in a thread finishes, the corresponding gradients are forwarded via the reusing queue to the CPU-side checkpointing process (Line 16), while the training process waits for the full gradient  $G_t$  (i.e., wait for handle set  $H_g$ ) (Line 6) to update the GPU model  $M^G_t$  (Line 7).

In the checkpointing process, gradients  $G^n_t$  streamed from the GPU are reused layer by layer (Line 9). The offloading thread pool  $P_s$  handles multiple layers in parallel (Line 10), snapshotting the layer-wise gradients into CPU memory as they become available (Line 19). This parallel snapshotting

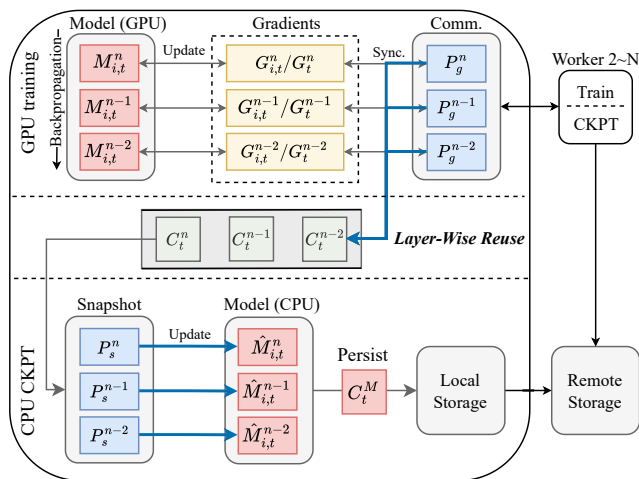


Fig. 9: Architecture of LowDiff+.

allows different layer gradients to be written concurrently to CPU memory, thereby better utilizing the available DRAM bandwidth. We initialize a CPU-resident replica  $M_t^C$  of the model parameters, aligned with the GPU state. After snapshotting (Line 11), reused gradients are applied to  $M_t^C$  to keep it synchronized with the GPU model  $M_t^G$  (Line 12). While gradients are snapshotted layer-by-layer, the CPU-side update (Line 12) is performed once the full gradient is aggregated. This is because the Adam optimizer requires the complete gradient to correctly update its internal states (e.g., momentum and variance). The updated model state in CPU memory serves as an in-memory checkpoint similar to Gemini [54]. Since such updates do not involve forward or backward computations, their execution on the CPU introduces negligible overhead. Persistence is performed asynchronously by checkpointing the CPU-maintained model replica (Line 13), rather than the raw gradients. The frequency of persistence is decided similarly to Checkfreq [36], which ensures maximal overlapping between the persist and update of the model in CPU. This design both avoids redundant storage of differential checkpoints and completely decouples persistence from GPU training, enabling fully asynchronous checkpointing with minimal interference to ongoing training.

**Recovery of LowDiff+.** When failure occurs, prior work categorizes failures into two broad types from the perspective of recovery: hardware failures and software failures. For hardware failures (e.g., GPU device crashes), the distributed training system must replace the failed machine with a new one. In this case, the in-memory training state is lost, so the recovery process must reload model states from persistent storage checkpoints, which can be time-consuming and increase wasted time.

In contrast, software failures (e.g., software bugs) only cause the training process to terminate. This design assumes the failure is confined to the training processes (e.g., a CUDA error or NaN loss) and does not corrupt the separate checkpointing process’s memory, thus leaving the CPU memory state of the checkpointing process intact. In such cases, recovery is achieved by reinitializing the training process and restoring the

## Algorithm 2 Reusing in LowDiff+

**Require:** GPU model state after the  $t$ -th iteration  $M_t^G$ , gradient of the  $n$ -th layer on node  $i$   $G_{i,t}^n$ , gradient communication and offload thread pools  $P_g$  and  $P_s$ , reusing queue  $Q$ , corresponding handle sets  $H_g$  and  $H_s$ .

```

1: function TRAINING PROCESS
2:   for all  $t$  do
3:     for all  $n$  do
4:        $G_{i,t}^n \leftarrow \text{Backward}(x_t^n)$ 
5:        $H_g.append(P_g.execute(\text{SYNC}, G_{i,t}^n))$ 
6:        $G_t \leftarrow H_g.wait()$ 
7:        $M_{t+1}^G \leftarrow M_t^G + \text{Adam}(o_t, G_t)$ 
8:   function CHECKPOINTING PROCESS
9:     while  $G_t^n \leftarrow Q.get$  do
10:       $H_s.append(P_s.execute(\text{SNAPSHOT}, G_t^n))$ 
11:       $G_t \leftarrow H_s.wait()$ 
12:       $M_{t+1}^C \leftarrow M_t^C + \text{Adam}(o_t, G_t)$ 
13:       $C_t^M \leftarrow \text{Save}(M_t^C)$ 
14:   function SYNC THREAD
15:      $G_t^n \leftarrow \text{Sync}(G_{i,t}^n)$ 
16:      $Q.put(G_t^n)$ 
17:     return  $G_t^n$ 
18:   function SNAPSHOT THREAD
19:      $G_t^n \leftarrow \text{Offload\_to\_cpu}(G_{i,t}^n)$ 
20:     return  $G_t^n$ 

```

preserved CPU-resident model state to the GPUs, leveraging in-memory checkpoints. This enables fast recovery under software failures, avoiding expensive checkpoint reloads and serving as a key optimization of LowDiff+.

## VII. IMPLEMENTATION

### A. Implementation of LowDiff

We implement LowDiff atop PyTorch [39], [40] and DeepSpeed [10], [44], consisting of three main modules: reusing queue (§V-A), batched gradient writing (§V-B), and optimal configuration (§V-C). In addition, a parallel recovery module accelerates recovery from a large number of differential checkpoints at high frequency.

**Reusing queue module.** Since Python’s GIL prevents true multi-threading, LowDiff uses `torch.multiprocessing` with the `spawn` method for process isolation. The compressed gradient Reusing Queue is implemented via `torch.multiprocessing.Queue()`, which (1) preserves checkpoint order and (2) leverages CUDA IPC for zero-copy GPU memory sharing.

**Batched gradient writing module.** Differential checkpoints are offloaded from GPU to CPU memory with `offload_to_cpu()` (non-blocking) and temporarily cached in a CPU buffer. GPU memory handles are released after offloading. Once the batch size is reached, checkpoints are aggregated (tensor addition or dictionary accumulation) and persisted to local or remote storage.

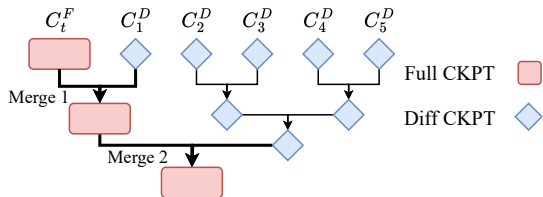


Fig. 10: Parallel Fast Recovery

**Optimal configuration module.** This module tunes full-checkpoint frequency and batch size based on Eq. (10). Starting from a default setup, it adapts to runtime metrics (failure rate, bandwidth) using stepwise adjustments to balance steady-state overhead and recovery cost, achieving efficient fault-tolerant checkpointing.

**Parallel recovery module.** Traditional recovery methods for differential checkpointing [15] use a *serial* process to merge multiple differential checkpoints with a base full checkpoint (see Equation (6)), whose the number of merge operations is  $n$  with given  $n$  differential checkpoints. Thus, we implement a *parallel* recovery module, which parallelizes the merge operations across full and differential checkpoints. Specifically, as shown in figure 10, it merges the earliest differential checkpoint  $C_1^D$  with the full checkpoint  $C_t^F$  while concurrently merging the subsequent differential checkpoints in pairs (i.e.,  $C_2^D$  and  $C_3^D$ ,  $C_4^D$  and  $C_5^D$ ). This parallelization reduces the number of merge operations between differential checkpoint and full checkpoint from  $n$  to  $\log n$ . In Figure 10, the number of merges between differential checkpoint and full checkpoint is 2 (the serial process has  $n = 5$  merges). Thus, the parallel recovery accelerates the overall recovery process over the traditional serial one.

### B. Implementation of LowDiff+

LowDiff+ is also implemented atop PyTorch [39], [40] and DeepSpeed [10], [44]. Since the checkpointing process is spawned from the training process, the model state in CPU is first initialized by a `copy.deepcopy()` of the GPU model to ensure consistency at the beginning. For gradient communication, we leverage Python’s `concurrent.futures` library and employ a `ThreadPoolExecutor` to assign each layer-wise gradient to a communication thread, ensuring parallel transmission. The snapshotting thread pool is implemented in the same manner, handling the writing of gradients into CPU memory.

To maintain the CPU-side model replica, we configure PyTorch intra-op parallelism via `torch.set_num_threads`, setting the number of threads to match the available CPU cores in order to maximize parallel efficiency. Importantly, the CPU update step only applies gradients to the model parameters without performing forward or backward propagation, which avoids heavy computation overhead and ensures that using CPU resources does not incur noticeable performance degradation. Finally, the persistence to storage is performed asynchronously, following a style similar to Checkfreq [36], thereby maximizing checkpointing throughput without interfering with GPU training.

GPU Type	GPU Mem	CPU Type
NVIDIA A100	80GB	Intel Xeon 8352V
NVIDIA V100S	32GB	Intel Xeon 4214

(a) GPU and CPU configurations of servers

Models	Datasets	Params
ResNet-50	Cifar-100	25.6M
ResNet-101	ImageNet	44.5M
VGG-16	Cifar-100	138.8M
VGG-19	ImageNet	143.7M
BERT-B	SQuAD	110M
BERT-L	SQuAD	334M
GPT2-S	WikiText-2	117M
GPT2-L	WikiText-103	762M

(b) Models and datasets used for evaluation

TABLE II: Experimental setup

## VIII. EVALUATION

In this section, we evaluate the efficiency of LowDiff to answer the following questions:

- How fast do LowDiff train under high checkpointing frequency compared to other methods? (Exp. 1)
- How fast do LowDiff+ train under non-compression scenarios? (Exp. 2)
- Can LowDiff and LowDiff+ achieve a shorter wasted time? (Exp. 3)
- Does LowDiff and LowDiff+ enable higher checkpointing frequency under bounded training speed? (Exp. 4)
- Does LowDiff and LowDiff+ accelerate the recovery process? (Exp. 5)
- Can LowDiff’s batched writes and offloaded batching reduce the checkpointing time and GPU memory cost? (Exp. 6)
- Can LowDiff reduce the storage overhead? (Exp. 7)
- Does LowDiff achieve frequent checkpointing under different compression ratios? (Exp. 8)
- Can LowDiff and LowDiff+ maintain high training efficiency under scenarios of more frequent failures and more GPUs? (Exp. 9-10)

### A. Experimental Setup

**Servers.** We assess the performance of LowDiff on two generations of NVIDIA GPUs, the A100 and V100S, with different CPU configurations. The specific server configurations are detailed in Table II(a). Each server is equipped with 4 GPUs, 512GB of system memory, and a 4TB Samsung SSD. Within a server, GPUs are interconnected via NVLink, while cross-server communication is performed over a 25Gbps Mellanox ConnectX-5 InfiniBand network. The A100 servers are equipped with PCIe Gen 4 interfaces, whereas the V100S servers use PCIe Gen 3 interfaces. All servers operate on Ubuntu 22.04 and are equipped with the following software libraries: Deepspeed-0.16.4, CUDA-12.4, NCCL-2.23.4, OpenMPI-4.0.5, Python-3.10.15, and PyTorch-2.6.0.

**Workloads.** We evaluate widely-used DNN models on tasks of image classification and natural language processing (NLP), including ResNet [20], VGG [49], Bert [14], and GPT-2 [41].

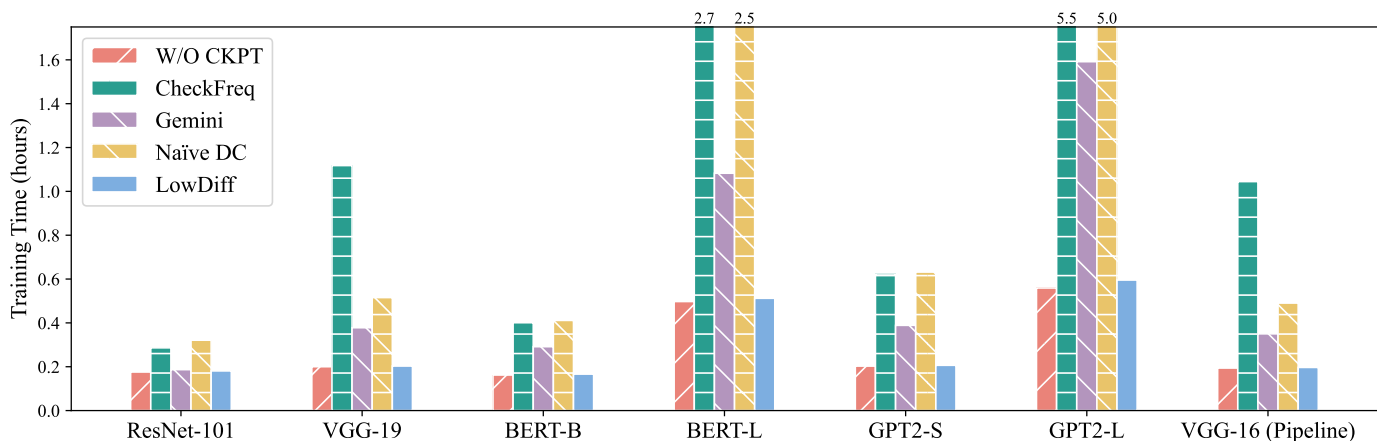


Fig. 11: (Exp. 1) Training time of different models with different checkpointing strategies.

The image classification models are evaluated on the CIFAR-100 [25] and ImageNet [12] datasets, and NLP models are evaluated on the SQuAD [43] and WikiText [33] datasets. The detailed configurations are shown in Table II(b). We use Adam [24] as the default optimizer. The training process uses sparsification compression with a common compress ratio  $\rho$  of 0.01 [3], [7], [18], [29], [35], [45]. We use default batching sizes and learning rates according to the original papers or standard practices. We also implement the LowDiff system on the VGG-16 model with pipeline parallelism provided in the DeepSpeedExamples [11].

**Baselines.** We evaluate two state-of-the-art checkpointing strategies: CheckFreq [36] and Gemini [54], as described in §II-B. The experiments follow the default configurations according to their original papers. Additionally, we assess the performance of the Naïve DC method, which computes the differences in model states between iterations and checkpoints these differentials, as Check-N-Run [15] does in recommendation systems.

### B. Performance Evaluation

**Experiment 1 (Training time of LowDiff).** We evaluate the training time of LowDiff under different checkpointing strategies on the previously introduced DNN models, with the checkpointing frequency set to once per iteration. The experiment is conducted in the presence of gradient compression. For each model, we run 1,000 training iterations on A100 servers and record the total training time. The *W/O CKPT* setting represents training without checkpointing, which serves as the upper bound of achievable training speed.

Figure 11 shows that the training time of LowDiff on all seven training tasks is close to that of *W/O CKPT* and significantly smaller than those of other solutions. Compared to *W/O CKPT*, LowDiff’s training time increases by only 2.4%-3.1%, while the other checkpointing methods’ training time increases by 8.1%-891%.

Specifically, we elaborate on LowDiff’s benefits over the other methods and analyze the reasons behind these benefits:

- Compared to CheckFreq and Gemini in GPT2-S, LowDiff reduces the training time by 68.2% and 46.1%, respectively.

We see that LowDiff significantly outperforms them under high frequency since LowDiff uses differential checkpointing with compression (compression ratio=0.01) to largely reduce the checkpoint sizes. Further, Gemini improves its training performance over CheckFreq by checkpointing to CPU memory, but the improvement is limited by its large checkpoint size.

- LowDiff’s performance improvement is more pronounced for larger models like BERT-L and GPT2-L. Compared to CheckFreq and Gemini in GPT2-L, LowDiff reduces the training time by 89.2% and 59.2%, respectively. This is because, as the model size increases, the advantage of the reduced checkpoint size of LowDiff becomes more dominant on the overall training time.
- Compared to Naïve DC in BERT-B, LowDiff reduces the training time by 60.5% due to its unique gradient reusing scheme, which reduces and even eliminates compression and transmission cost of Naïve DC, confirming the efficiency of our reusing idea in §III-C. It should be noted that, in comparison with CheckFreq and Gemini, Naïve DC fails to demonstrate the advantage of its reduced checkpoint size due to its high costs.
- LowDiff’s performance improvement remains significant in pipeline parallelism. Compared to Naïve DC, CheckFreq, and Gemini in VGG16 with pipeline parallelism, LowDiff reduces the training time by 70.8%, 60.9%, and 36.9%, respectively. The reason is that LowDiff’s efficient high-frequency DC relies on the core technique that reuses the compressed gradients, which are computed during training and still exist in pipeline-parallelism-based training systems. Thus, reusing compressed gradients and pipeline parallelism can be combined for training efficiency. Our future work will explore the efficiency of such a combination.

**Experiment 2 (Training time of LowDiff+).** To isolate the impact of gradient compression, we further evaluate the training time of LowDiff+ in a setting without gradient compression. All other experimental configurations, including the checkpointing frequency (per iteration), the selected DNN models, the number of training iterations (1,000), and the hardware environment (A100 servers), remain identical to Exp. 1.

Figure 12 shows that the training time of LowDiff+ across

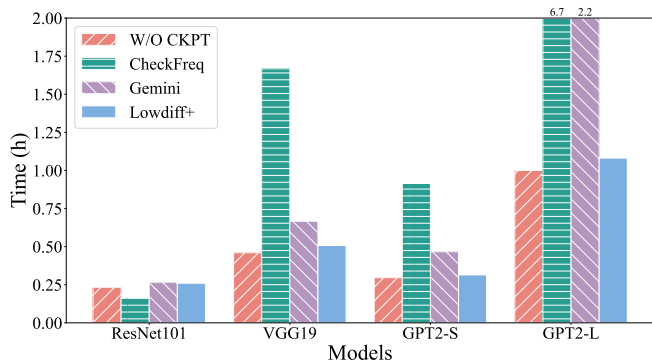


Fig. 12: (Exp. 2) Training time without compression.

all tasks exhibits a slight increase compared to the W/O CKPT baseline, yet it remains significantly lower than that of other checkpointing solutions. Specifically, **LowDiff+**'s training time increases by 7.2%–9.1% relative to W/O CKPT. As expected, this overhead is higher than the 2.4%–3.1% observed for **LowDiff** in Exp. 1. This increase represents the necessary and expected performance trade-off for handling uncompressed, high-precision gradients, which was the primary motivation for the **LowDiff+** design. The overhead is mainly due to frequent and large-volume gradient transfers between GPU and CPU memory, occupying PCIe bandwidth.

Despite this minor overhead, in the high-frequency checkpointing scenario without gradient compression, **LowDiff+** consistently achieves the lowest training time among all checkpointing methods. For the GPT2-L training task, it reduces the training time by 51.8% compared to Gemini and by 81.7% compared to CheckFreq, demonstrating its superior efficiency in settings where frequent non-compression checkpoints are required.

**Experiment 3 (Wasted time).** We evaluate the wasted time of various checkpointing methods in the event of failures. Failures were simulated during training by adhering to a fixed Mean Time Between Failures (MTBF) metric. Using three MTBF values at 0.5, 1, and 2 [19], respectively, we evaluate the wasted time of Naïve DC, CheckFreq, Gemini, and **LowDiff** when training GPT2-S. Note that **LowDiff**'s checkpointing optimal configuration is obtained based on Equation (5) in §V-C. For **LowDiff+**, we evaluate its wasted time under both software and hardware failures, where the corresponding checkpoints can be accessed through snapshot and persist (**LowDiff+** (S) and **LowDiff+** (P), respectively).

Figure 13 shows that the wasted time gap between **LowDiff** and other checkpointing methods keeps increasing as failures become more frequent, while **LowDiff** maintains the lowest wasted time. When the MTBF decreases from 2 to 0.5 (lower MTBF means more frequent failures), the gap between **LowDiff** and Gemini increases from 0.061h to 0.145h. This is because **LowDiff** tunes the full checkpointing frequency and batching size to approach the optimal configuration of checkpointing, while other methods' wasted time is greatly influenced by the different parameters. The results confirm the efficiency of **LowDiff** in the event of failures.

For **LowDiff+**, the wasted time due to software failures is

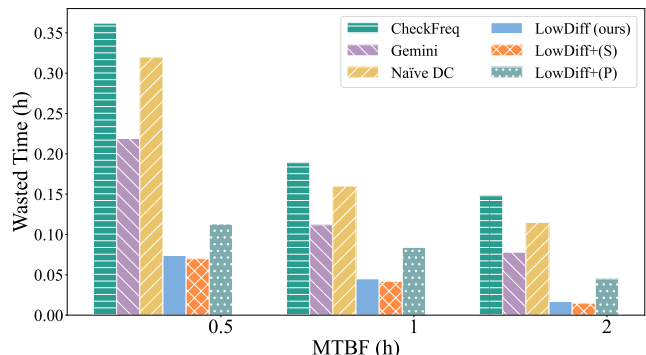


Fig. 13: (Exp. 3) Wasted time under different MTBFs.

3.7%–5.1% lower than that of **LowDiff**. This improvement comes from **LowDiff+**'s in-memory checkpointing, which enables fast recovery using the full model state stored in CPU memory. The detailed recovery times of **LowDiff+** (S) are presented in Exp. 5. In contrast, the wasted time from hardware failures is slightly higher than that of **LowDiff**, due to **LowDiff+**'s lower checkpointing frequency, but still lower than that of CheckFreq and Gemini. Details of the checkpointing frequency for **LowDiff+** (S) and **LowDiff+** (H) are presented in Exp. 6.

**Experiment 4 (Checkpointing frequency).** To evaluate the maximum checkpointing frequency that each method can achieve under bounded training speed (set as 3.5%, as the degraded speed of model training is required to be less than 3.5% in Microsoft's study [36]), we evaluate the highest checkpointing frequency of different methods. We denote **LowDiff+**'s in-memory checkpointing as **LowDiff+** (S) and its persistence as **LowDiff+** (P).

Figure 14 shows that compared to other methods, **LowDiff** can achieve the checkpointing frequency every iteration (i.e., the checkpointing frequency equals one) for different widely-used models under the bounded training speed.

**LowDiff+** (S) also performs per-iteration in-memory checkpointing, enabled by its efficient layer-wise gradient reuse and snapshotting approach. **LowDiff+** (P) achieves per-iteration persistence frequency in smaller models such as ResNet-101, but increases to 3 iterations for larger models like GPT2-L due to the limited bandwidth of SSDs. Nevertheless, its checkpointing intervals remain the shortest compared to Naïve DC, CheckFreq, and Gemini.

Intervals of Naïve DC grow significantly with model size, increasing from every 2 iterations to every 8. Gemini only supports per-iteration checkpointing on ResNet-101, and its interval increases to every 4 iterations for GPT2-L and BERT-L. CheckFreq consistently maintains an interval of 10 iterations. These results validate our motivation that **LowDiff** can support high-frequency checkpointing without stalling training progress.

**Experiment 5 (Recovery time).** We evaluate the recovery time of different recovery strategies under different full checkpointing frequency in GPT2-S. We compare traditional checkpointing without differential checkpoint (Baseline) (i.e., `Torch.save` [39]), Naïve DC, **LowDiff** with parallel recov-

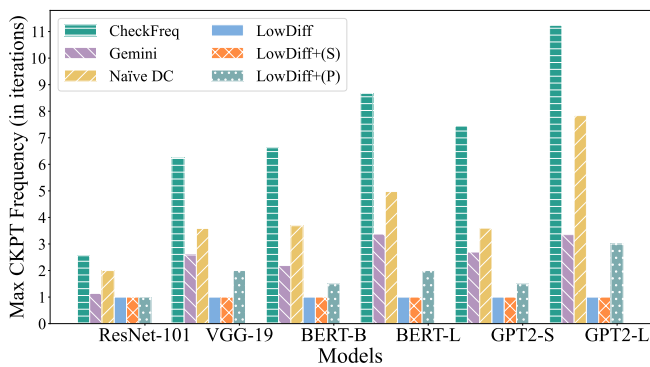


Fig. 14: (Exp. 4) Maximum checkpointing frequency.

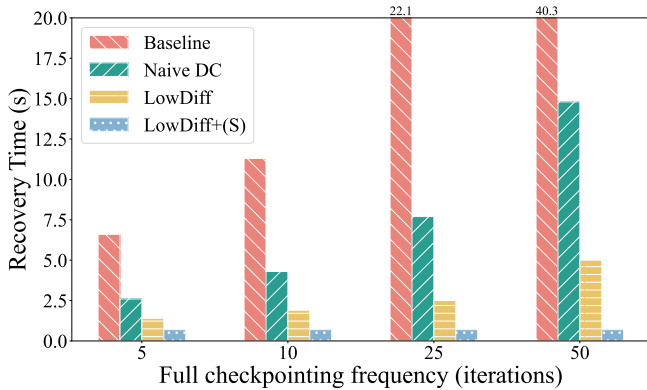


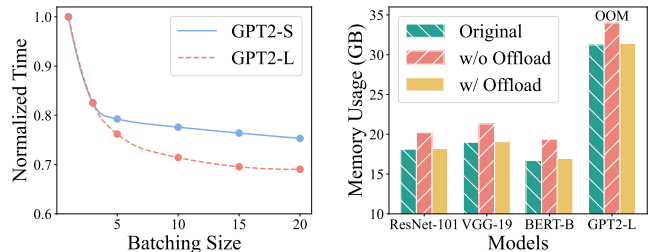
Fig. 15: (Exp. 5) Recovery time of different methods.

ery (see §VII), and **LowDiff+** from software failures (**LowDiff+**(S) for short). Note that recovery from hardware failures in **LowDiff+** is the same as in the baseline, since both reload the model from storage and resume training from the last persisted checkpoint, as determined by the checkpointing frequency.

Figure 15 shows that the recovery time of **LowDiff** with parallel recovery is consistently smaller than that of **Baseline** and **Naïve DC**. For example, when the full checkpointing frequency is 10 iterations, **LowDiff** with parallel recovery reduces recovery time by 83.2% and 55.8% compared with **Baseline** and **Naïve DC**, respectively. In contrast, **LowDiff+** achieves the shortest recovery time overall, as it performs *in-memory differential checkpointing* at every iteration. By avoiding reloads from persistent storage and directly applying in-memory states, **LowDiff+** delivers  $9.4\times$ – $57.1\times$  faster recovery than **Baseline** across full checkpointing frequencies from 5 to 50.

**Experiment 6 (Checkpointing time reduction and GPU memory reduction).** To evaluate the reduction in average checkpointing time achieved by the batched write optimization proposed in §V-B, we conduct experiments on various models with different batching sizes. Figure 16a shows that the batched write strategy significantly reduces the average time required to write differential checkpoints, with a maximum reduction of 30.9% when the batching size is 20 during GPT2-S training.

The batching strategy effectively accelerates the checkpoint writing process. After tuning the batching frequency with the configuration strategies discussed in §V-A, the optimization



(a) Average checkpointing time under different batch sizes (b) GPU memory consumption w/o and w/ offloaded batching

Fig. 16: (Exp. 6) CKPT time and GPU memory reduction.

Model	Full CKPT	Naïve DC	LowDiff
ResNet-101	511M	346M	34M
VGG-19	1.7G	1.13G	109M
BERT-B	1.3G	930M	82M
BERT-L	3.8G	2.55G	239M
GPT2-S	1.4G	946M	92M
GPT2-L	8.7G	5.7G	541M

TABLE III: (Exp. 7) Storage overhead of checkpoints.

can adapt to different compression ratios and minimize the impact on training performance.

Additionally, we also evaluate the reduction of GPU memory achieved by the batching offloaded in CPU §V-B. Figure 16b shows that the GPU memory usage will increase by 10% – 12% without offloaded batching, especially for GPT2-L, potentially leading to memory exhaustion. In contrast, the GPU memory usage will return to the original state with the help of offloaded batching.

**Experiment 7 (Storage overhead).** We evaluate the storage overhead of checkpoints for various checkpointing methods and various DNN models, where **CheckFreq** and **Gemini** only have full checkpoints (called **Full CKPT**), **Naïve DC** and **LowDiff** have full and differential checkpoints. As shown in Table III, compared to full checkpoints, **Naïve DC** reduces the storage overhead by 34.4% due to the compression technique used in the model parameters.

Compared to **Naïve DC**, **LowDiff** further reduces the storage overhead by 90.5%. Because **LowDiff** utilizes compressed gradients to construct differentials for both model parameters and optimizer parameters (Finding 2 in §III-B), while **Naïve DC** (**Check-N-Run** [15]) does not apply sparsification compression to the optimizer parameters within differential checkpoints, resulting in the optimizer occupying the majority of the checkpoint space. The result ensures our motivation that **LowDiff** can significantly reduce the checkpoint size and thus lower the storage cost.

**Experiment 8 (Impact of compression ratio  $\rho$ ).** We evaluate the impact of different compression ratios  $\rho$  on the checkpoint frequency of GPT2-L and GPT2-S training. The compression ratio  $\rho$  varies from 0.1 to 0.001, consistent with the ranges commonly used in prior work [29], [35].

As shown in Figure 17, **LowDiff** enables per-iteration checkpointing for GPT2-S training across the entire range of  $\rho \in [0.001, 0.1]$  due to its smaller enough gradient size

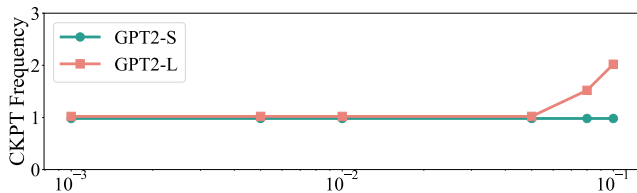


Fig. 17: (Exp. 8) Impact of Compression Ratio  $\rho$ .

for checkpointing to be overlapped with training within one iteration. For GPT2-L, LowDiff supports per-iteration checkpointing when  $\rho \in [0.001, 0.075]$ , while at  $\rho = 0.1$ , the checkpoint frequency increases to 2 iterations because the increasing gradient size makes the checkpointing take two iterations to be overlapped with training. The result shows LowDiff ensures frequent checkpointing (intervals  $\leq 3$  iterations) under the common compression ratio.

### C. System Scalability

We test the scalability of LowDiff and LowDiff+ on V100 servers in scenarios with frequent failures and more GPUs to demonstrate the robustness and efficiency of LowDiff and LowDiff+.

**Experiment 9 (Scaling to frequent failures).** We conduct experiments on the performance of LowDiff and LowDiff+ in extreme scenarios characterized by more frequent failures of the training process with MTBF ranging from 0.1 to 5 hours. Using the effective training time ratio as defined in Gemini [54], which measures the percentage of time spent on productive training progress within a given period of time, we evaluate the effective training time ratios of `Torch.save` (baseline), CheckFreq, Gemini, LowDiff, and LowDiff+. Note that LowDiff+ has two recovery modes: LowDiff+ (S) for software failures (recovering from CPU memory) and LowDiff+ (P) for hardware failures (recovering from persistent storage).

Figure 18 demonstrates that LowDiff+ (S) consistently achieves the highest effective training time ratio across all scenarios, especially under environments with frequent failures. This is because its near-instantaneous recovery from in-memory checkpoints (as shown in Exp. 5) almost completely eliminates recovery overhead, compensating for its slightly higher steady-state overhead compared to LowDiff. LowDiff achieves the second-highest ratio. LowDiff+ (P) also consistently outperforms the other baselines, though its reliance on slower disk-based recovery places it slightly below LowDiff. For example, when the MTBF is set to 0.3 hours, LowDiff+ (S) leads with an effective training time ratio of 94.0%, followed closely by LowDiff at 92%. LowDiff+ (P) achieves 86.8%, which is still significantly higher than Gemini (81%) and Checkfreq (75.9%). These results highlight the robustness of our approaches, with LowDiff+ (S) offering the best performance for common software failures.

**Experiment 10 (Scaling to more GPUs).** We evaluate the training performance by varying the number of GPUs used in the training process, using the same effective training time ratio metric as in Experiment 7. As the number of GPUs increases, the probability of failures in the cluster also rises

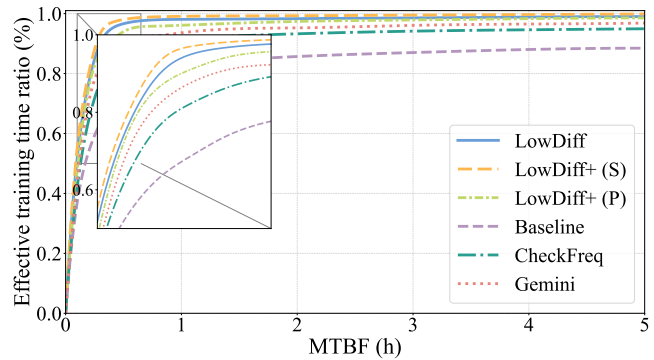


Fig. 18: (Exp. 9) Training under frequent failures.

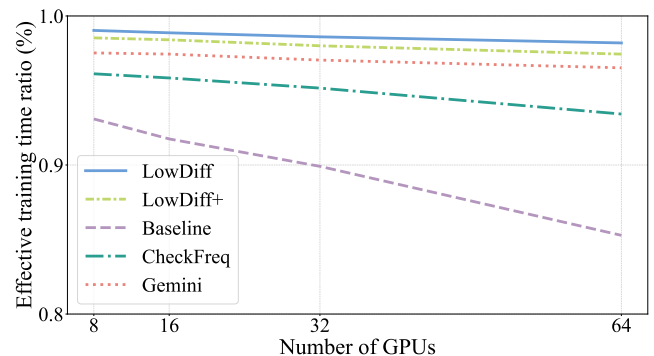


Fig. 19: (Exp. 10) Training with different number of GPUs.

[19]. We conduct experiments with 8, 16, 32, and 64 GPUs, respectively, and measure the effective training time ratio of `Torch.save` (baseline), CheckFreq, Gemini, LowDiff, and LowDiff+.

Figure 19 shows that, as the number of GPUs increases, the effective training time ratio decreases; however, LowDiff still maintains a 98% proportion of the effective training time ratio, and LowDiff+ achieves 96%, while the metric for the other method declines rapidly and can only reach around 90%. This highlights the strong potential of LowDiff and LowDiff+ in large-scale training.

## IX. CONCLUSION

LowDiff is an efficient frequent checkpointing framework that addresses the challenges of the high costs of differential checkpointing by reusing the compressed gradients generated during training. LowDiff also designs a batched gradient writing optimization scheme and an optimal configuration tuning scheme. To enhance the gradient reuse strategy in non-compression scenarios, we design LowDiff+. LowDiff+ uses a layer-wise gradient reusing and snapshotting strategy and a CPU-based synchronous persistence strategy, thus enabling checkpointing to decouple from training. Our experiments on a variety of models and GPU generations demonstrate the efficiency of LowDiff and LowDiff+ in terms of the training time, wasted time, checkpointing time, and recovery time under the high-frequency checkpointing scenarios.

## REFERENCES

- [1] Martín Abadi, Paul Barham, Jianmin Chen, Zhifeng Chen, Andy Davis, Jeffrey Dean, Matthieu Devin, Sanjay Ghemawat, Geoffrey Irving, and Michael Isard. Tensorflow: a system for large-scale machine learning. In *12th USENIX symposium on operating systems design and implementation (OSDI 16)*, pages 265–283, 2016.
- [2] Sanad Aburass and Osama Dorgham. Performance evaluation of swin vision transformer model using gradient accumulation optimization technique. In *Proceedings of the Future Technologies Conference (FTC) 2023, Volume 4*, pages 56–64, 2023.
- [3] Alham Fikri Aji and Kenneth Heafield. Sparse communication for distributed gradient descent. *arXiv preprint arXiv:1704.05021*, 2017.
- [4] Dan Alistarh, Demjan Grubic, Jerry Li, Ryota Tomioka, and Milan Vojnovic. Qsgd: Communication-efficient sgd via gradient quantization and encoding. *Advances in neural information processing systems*, 30, 2017.
- [5] Dan Alistarh, Demjan Grubic, Jerry Li, Ryota Tomioka, and Milan Vojnovic. Qsgd: Communication-efficient sgd via gradient quantization and encoding. In I. Guyon, U. Von Luxburg, S. Bengio, H. Wallach, R. Fergus, S. Vishwanathan, and R. Garnett, editors, *Advances in Neural Information Processing Systems*, volume 30. Curran Associates, Inc., 2017.
- [6] Tom Brown, Benjamin Mann, Nick Ryder, Melanie Subbiah, Jared D Kaplan, Prafulla Dhariwal, Arvind Neelakantan, Pranav Shyam, Girish Sastry, and Amanda Askell. Language models are few-shot learners. *Advances in neural information processing systems*, 33:1877–1901, 2020.
- [7] Chang Chen, Min Li, and Chao Yang. bbtok: Bandwidth-aware sparse allreduce with blocked sparsification for efficient distributed training. In *2023 IEEE 43rd International Conference on Distributed Computing Systems (ICDCS)*, pages 1–11. IEEE, 2023.
- [8] Menglei Chen, Yu Hua, Rong Bai, and Jianming Huang. A cost-efficient failure-tolerant scheme for distributed dnn training. In *2023 IEEE 41st International Conference on Computer Design (ICCD)*, pages 150–157. IEEE, 2023.
- [9] Ping Chen, Shuibing He, Xuechen Zhang, Shuaiben Chen, Peiyi Hong, Yanlong Yin, Xian-He Sun, and Gang Chen. Cswap: A self-tuning compression framework for accelerating tensor swapping in gpus. In *2021 IEEE International Conference on Cluster Computing (CLUSTER)*, pages 271–282. IEEE, 2021.
- [10] DeepSpeed. <https://github.com/deepspeedai/DeepSpeed/>.
- [11] DeepSpeedExample. <https://github.com/deepspeedai/DeepSpeedExamples/>.
- [12] Jia Deng, Wei Dong, Richard Socher, Li-Jia Li, Kai Li, and Li Fei-Fei. Imagenet: A large-scale hierarchical image database. In *2009 IEEE conference on computer vision and pattern recognition*, pages 248–255. Ieee, 2009.
- [13] Tim Dettmers. 8-bit approximations for parallelism in deep learning. *arXiv preprint arXiv:1511.04561*, 2015.
- [14] Jacob Devlin, Ming-Wei Chang, Kenton Lee, and Kristina Toutanova. Bert: Pre-training of deep bidirectional transformers for language understanding. *arXiv preprint arXiv:1810.04805*, 2018.
- [15] Assaf Eisenman, Kiran Kumar Matam, Steven Ingram, Dheevatsa Mudigere, Raghuraman Krishnamoorthi, Krishnakumar Nair, Misha Smelyanskiy, and Murali Annaram. Check-n-run: A checkpointing system for training deep learning recommendation models. In *19th USENIX Symposium on Networked Systems Design and Implementation (NSDI 22)*, pages 929–943, 2022.
- [16] Fartash Faghri, Iman Tabrizian, Ilija Markov, Dan Alistarh, Daniel M Roy, and Ali Ramezani-Kebrya. Adaptive gradient quantization for data-parallel sgd. *Advances in neural information processing systems*, 33:3174–3185, 2020.
- [17] Jiarui Fang, Haohuan Fu, Guangwen Yang, and Cho-Jui Hsieh. Redsync: reducing synchronization bandwidth for distributed deep learning training system. *Journal of Parallel and Distributed Computing*, 133:30–39, 2019.
- [18] Jiawei Fei, Chen-Yu Ho, Atal N Sahu, Marco Canini, and Amedeo Sapia. Efficient sparse collective communication and its application to accelerate distributed deep learning. In *Proceedings of the 2021 ACM SIGCOMM 2021 Conference*, pages 676–691, 2021.
- [19] Tanmaey Gupta, Sanjeev Krishnan, Rituraj Kumar, Abhishek Vijeev, Bhargav Gulavani, Nipun Kwatra, Ramachandran Ramjee, and Muthian Sivathanu. Just-in-time checkpointing: Low cost error recovery from deep learning training failures. In *Proceedings of the Nineteenth European Conference on Computer Systems*, pages 1110–1125, 2024.
- [20] Kaiming He, Xiangyu Zhang, Shaoqing Ren, and Jian Sun. Deep residual learning for image recognition. In *Proceedings of the IEEE conference on computer vision and pattern recognition*, pages 770–778, 2016.
- [21] John L Hennessy and David A Patterson. *Computer architecture: a quantitative approach*. Elsevier, 2011.
- [22] Joeri R. Hermans, Gerasimos Spanakis, and Rico Möckel. Accumulated gradient normalization. In *Proceedings of the Ninth Asian Conference on Machine Learning*, volume 77, pages 439–454, 2017.
- [23] Myeongjae Jeon, Shivaram Venkataraman, Amar Phanishayee, Junjie Qian, Wencong Xiao, and Fan Yang. Analysis of {Large-Scale}{Multi-Tenant}{GPU} clusters for {DNN} training workloads. In *2019 USENIX Annual Technical Conference (USENIX ATC 19)*, pages 947–960, 2019.
- [24] Diederik P. Kingma and Jimmy Ba. Adam: A method for stochastic optimization. In *ICLR (Poster)*, 2015.
- [25] Alex Krizhevsky and Geoffrey Hinton. Learning multiple layers of features from tiny images. *University of Toronto*, 2009.
- [26] Mu Li, David G Andersen, Alexander J Smola, and Kai Yu. Communication efficient distributed machine learning with the parameter server. *Advances in Neural Information Processing Systems*, 27, 2014.
- [27] Mu Li, Li Zhou, Zichao Yang, Aaron Li, Fei Xia, David G Andersen, and Alexander Smola. Parameter server for distributed machine learning. In *Big learning NIPS workshop*, volume 6. Lake Tahoe, CA, 2013.
- [28] Shen Li, Yanli Zhao, Rohan Varma, Omkar Salpekar, Pieter Noordhuis, Teng Li, Adam Paszke, Jeff Smith, Brian Vaughan, and Pritam Damania. Pytorch distributed: Experiences on accelerating data parallel training. *arXiv preprint arXiv:2006.15704*, 2020.
- [29] Shigang Li and Torsten Hoefler. Near-optimal sparse allreduce for distributed deep learning. In *Proceedings of the 27th ACM SIGPLAN Symposium on Principles and Practice of Parallel Programming*, pages 135–149, 2022.
- [30] Yujun Lin, Song Han, Huizi Mao, Yu Wang, and William J Dally. Deep gradient compression: Reducing the communication bandwidth for distributed training. *arXiv preprint arXiv:1712.01887*, 2017.
- [31] Ahmed M Abdelmoniem, Ahmed Elzanaty, Mohamed-Slim Alouini, and Marco Canini. An efficient statistical-based gradient compression technique for distributed training systems. *Proceedings of Machine Learning and Systems*, 3:297–322, 2021.
- [32] Avinash Maurya, Robert Underwood, M Mustafa Rafique, Franck Cappello, and Bogdan Nicolae. Datasates-llm: Lazy asynchronous checkpointing for large language models. In *Proceedings of the 33rd International Symposium on High-Performance Parallel and Distributed Computing*, pages 227–239, 2024.
- [33] Stephen Merity, Caiming Xiong, James Bradbury, and Richard Socher. Pointer sentinel mixture models. *arXiv preprint arXiv:1609.07843*, 2016.
- [34] Meta. Opt-175b logbook. [https://github.com/facebookresearch/metaseq/blob/main/projects/OPT/chronicles/OPT175B\\_Logbook.pdf/](https://github.com/facebookresearch/metaseq/blob/main/projects/OPT/chronicles/OPT175B_Logbook.pdf/).
- [35] Zhangqiang Ming, Yuchong Hu, Wenxiang Zhou, Xinjue Zheng, Chenxuan Yao, and Dan Feng. Adtopk: All-dimension top-k compression for high-performance data-parallel dnn training. In *Proceedings of the 33rd International Symposium on High-Performance Parallel and Distributed Computing*, pages 135–147, 2024.
- [36] Jayashree Mohan, Amar Phanishayee, and Vijay Chidambaram. Check-freq: Frequent, fine-grained dnn checkpointing. In *19th USENIX Conference on File and Storage Technologies (FAST 21)*, pages 203–216, 2021.
- [37] OpenAI. Chatgpt. <https://openai.com/index/chatgpt/>.
- [38] OpenAI. GPT-4 technical report, 2024.
- [39] Adam Paszke, Sam Gross, Francisco Massa, Adam Lerer, James Bradbury, Gregory Chanan, Trevor Killeen, Zeming Lin, Natalia Gimelshein, and Luca Antiga. Pytorch: An imperative style, high-performance deep learning library. *Advances in neural information processing systems*, 32, 2019.
- [40] Pytorch. <https://github.com/pytorch/pytorch>.
- [41] Alec Radford, Jeffrey Wu, Rewon Child, David Luan, Dario Amodei, and Ilya Sutskever. Language models are unsupervised multitask learners. *OpenAI blog*, 1(8):9, 2019.
- [42] Samyam Rajbhandari, Jeff Rasley, Olatunji Ruwase, and Yuxiong He. Zero: Memory optimizations toward training trillion parameter models. In *SC20: International Conference for High Performance Computing, Networking, Storage and Analysis*, pages 1–16. IEEE, 2020.
- [43] Pranav Rajpurkar, Robin Jia, and Percy Liang. Know what you don't know: Unanswerable questions for squad. *CoRR*, abs/1806.03822, 2018.
- [44] Jeff Rasley, Samyam Rajbhandari, Olatunji Ruwase, and Yuxiong He. Deepspeed: System optimizations enable training deep learning models with over 100 billion parameters. In *Proceedings of the 26th ACM*

- SIGKDD International Conference on Knowledge Discovery & Data Mining*, pages 3505–3506, 2020.
- [45] Cédric Renggli, Saleh Ashkboos, Mehdi Aghagolzadeh, Dan Alistarh, and Torsten Hoefler. Sparcml: High-performance sparse communication for machine learning. In *Proceedings of the International Conference for High Performance Computing, Networking, Storage and Analysis*, pages 1–15, 2019.
- [46] Alexander Sergeev and Mike Del Balso. Horovod: fast and easy distributed deep learning in tensorflow, 2018.
- [47] Shaohuai Shi, Zhenheng Tang, Qiang Wang, Kaiyong Zhao, and Xiaowen Chu. Layer-wise adaptive gradient sparsification for distributed deep learning with convergence guarantees. *arXiv preprint arXiv:1911.08727*, 2019.
- [48] Shaohuai Shi, Qiang Wang, Kaiyong Zhao, Zhenheng Tang, Yuxin Wang, Xiang Huang, and Xiaowen Chu. A distributed synchronous sgd algorithm with global top-k sparsification for low bandwidth networks. In *2019 IEEE 39th International Conference on Distributed Computing Systems (ICDCS)*, pages 2238–2247. IEEE, 2019.
- [49] Karen Simonyan and Andrew Zisserman. Very deep convolutional networks for large-scale image recognition. *arXiv preprint arXiv:1409.1556*, 2014.
- [50] Jaeyong Song, Jinkyu Yim, Jaewon Jung, Hongsun Jang, Hyung-Jin Kim, Youngsok Kim, and Jinho Lee. Optimus-cc: Efficient large nlp model training with 3d parallelism aware communication compression. In *Proceedings of the 28th ACM International Conference on Architectural Support for Programming Languages and Operating Systems, Volume 2*, pages 560–573, 2023.
- [51] Sebastian U Stich, Jean-Baptiste Cordonnier, and Martin Jaggi. Sparsified sgd with memory. *Advances in neural information processing systems*, 31, 2018.
- [52] Foteini Strati, Michal Friedman, and Ana Klimovic. Pccheck: Persistent concurrent checkpointing for ml. In *Proceedings of the 30th ACM International Conference on Architectural Support for Programming Languages and Operating Systems, Volume 1*, pages 811–827, 2025.
- [53] Guanhua Wang, Olatunji Ruwase, Bing Xie, and Yuxiong He. Fastpersist: Accelerating model checkpointing in deep learning, 2024.
- [54] Zhuang Wang, Zhen Jia, Shuai Zheng, Zhen Zhang, Xinwei Fu, TS Eugene Ng, and Yida Wang. Gemini: Fast failure recovery in distributed training with in-memory checkpoints. In *Proceedings of the 29th Symposium on Operating Systems Principles*, pages 364–381, 2023.
- [55] Ru Zhang, Wencong Xiao, Hongyu Zhang, Yu Liu, Haoxiang Lin, and Mao Yang. An empirical study on program failures of deep learning jobs. in 2020 ieee/acm 42nd international conference on software engineering (icse). *IEEE*, 115961170, 2020.
- [56] Yanli Zhao, Andrew Gu, Rohan Varma, Liang Luo, Chien-Chin Huang, Min Xu, Less Wright, Hamid Shojanazeri, Myle Ott, Sam Shleifer, Alban Desmaison, Can Balioglu, Pritam Damania, Bernard Nguyen, Geeta Chauhan, Yuchen Hao, Ajit Mathews, and Shen Li. Pytorch fsdp: Experiences on scaling fully sharded data parallel. *Proceedings of the VLDB Endowment*, 16:3848–3860, 09 2023.